CHAPTER 6
THE EFFECT OF COOPERATIVE CHARGING ON FILTRATION PROPERTIES OF ELECTRICALLY DISSIMILAR ELECTROSPUN NANOFIBERS OF POLYMERS[†]

6.1 Chapter Summary

Electrical charging and residual charge decay of electrospun nonwoven webs comprised of two electrically dissimilar polymers were studied in an effort to investigate their filtration properties. Electrospinning of polystyrene (PS) and polyacrylonitrile (PAN) was performed by utilizing three different approaches to produce thin fibrous webs: PAN and PS were electrospun individually in a 'single component' fashion; in a 'layer-by-layer' configuration; and simultaneously in a side-by-side 'bicomponent' apparatus to yield bicomponent fibers. During electrospinning of the PS and PAN polymer solutions, the fibers were found to become positively charged when a positive voltage (+15kV) was applied to the solution-filled spinning nozzle and were found to become negatively charged when a negative voltage (-15kV) was applied to the spinning nozzle. This study allowed the examination of the effect of the electrospinning on inducing charges of different polarity on two electrically dissimilar polymers, viz. PAN and PS, and to determine the effect of the three types of web constructions ('single component', 'layer-by-layer' and 'bicomponent') on charge retention and filtration properties of the resulting nanofibers. It was found that single, multilayered, and bicomponent webs retained surface charges in the thousands of volts that diminished very little over a 20-hour period, but eventually bled off while in storage for three months. Filtration properties were found to be exceptionally high for some, but not all, electrospun samples; filtration was found to have a weak dependence on both surface charge and web geometrical factors, particularly the fiber diameter, that influence pressure drop of the aerosol.

Keywords: Electrospinning, aerosol penetration, filtration, efficiency

[†] H. Schreuder-Gibson, P. Gibson, P. Tsai, P. Gupta, G. Wilkes, manuscript submitted to *International Nonwovens Journal*

6.2 Introduction

The method of electrospinning polymer fibers from solution has been described in many patents and research papers since the 1930's.[1-6] The technique involves the ejection of a jet from the surface of a charged polymer solution when the applied electric field strength (and consequently the electrostatic repulsion on the surface of the fluid) overcomes the surface tension. This jet rapidly travels to the grounded collector target located at some distance from the charged polymer solution under the influence of the electric field. Solidified polymer filaments are collected on the target as the jet dries.[7-12] Although the phenomenon of electrospun fibers ejecting from the surface of a charged polymer solution is still being defined through engineering studies and modeling of the electrospinning process,[13-18] practical use has been made of these ultrafine fibers for filtration.

It is well known that in a typical aerosol filtration test, the porosity of the filters plays an important role. The velocity of the aerosol inside a filter is dependent on the porosity of the filters. Infact, the relationship between the aerosol velocity and porosity is given by:[19]

$$\mathbf{U} = \frac{\mathbf{Q}}{\mathbf{A}.\beta} \qquad 6.1$$

where U is the aerosol velocity, Q is the volumetric flow rate, A is the cross-sectional area of the filter exposed to the entering mainstream and β is the porosity of the filter. As filtration efficiency is inversely proportional to the aerosol velocity, it is clear that the filtration efficiency relates inversely with the porosity of the filters. In addition, the porosity of the filters depends on the fiber diameter, thickness of the filter, and the geometrical arrangement of fibers within the filter that in turn governs the packing density of the fibers. Moreover, the single-fiber filtration efficiency (FE) depends on aerosol particle size, fiber diameter, initial velocity of the aerosol particles and surface charges on the fiber and aerosol particles.[19] Studies involving fibers made from conventional melt and spinning techniques, where fiber diameters usually run from tens of microns and more, have indicated that filtration efficiency is inversely proportional to fiber diameter and directly proportional to the attractive electrostatic forces induced due to charged aerosol or fiber surfaces. To date, systematic studies involving charged

electrospun submicron fibers have not been conducted where the effect of fiber diameter and surface charges on filtration properties has been ascertained. In the past, some of the coauthors of this study investigated the effects of electrical charges on the ejected jet on target coverage during electrospinning.[20] They found that fibers of different polymers would repel each other and would not intermingle into a single region of mixed fibers on a charged collection surface. In addition, polystyrene (PS), a good electrical insulator, was found to carry a relatively high charge potential of -800V immediately after electrospinning, which decayed to about 200 volts after 100 minutes (Note that the electrospinning of PS was carried out from a 20wt% solution in 80/20 THF/DMF, -15 kV and at a distance of 30 cm between the grounded target and the charged electrode). In particular, among the different polymers investigated, the charge retention on the electrospun PS and polyacrylonitrile (PAN) was notable. Based on those results, we decided to further investigate the effect of fiber charging and web construction on residual charge decay and filtration efficiency of the electrospun webs over time. The following study examined the charging and filtration effects from three types of web construction designed to produce cooperative charging between dissimilarly charged fibers: single component fibers of PS and PAN electrospun separately, bicomponent fibers of PS and PAN that were electrospun simultaneously, and individual layers of fibers of PS and PAN carrying different charge polarity were electrospun in subsequent time intervals on the same substrate to give a two-layer or four-layer mat. In order to accomplish bicomponent electrospinning, it was necessary to use a special spinneret designed for cospinning fibers to overcome the charge interference between dissimilar fibers that had previously been observed. The bicomponent spinning system used in this study had been designed and previously reported to produce bicomponent electrospun fibers of two different polymers into a single web.[21]

The overall objective of this work was to determine whether a bicomponent fiber web containing fibers of identical charge polarity would produce a cooperative charging effect causing retention of electrical charge over a long period of time, as in the case of triboelectrically charged fabrics, or whether a multilayered mat of oppositely charged fiber layers would provide extended electrical charge retention for high filtration efficiency. Two polymers were selected as electrically dissimilar materials for this

experiment: modacrylic is reported to gain charge when carded in triboelectric filter applications,[22] so we used an acrylic polymer, PAN, for our study; in addition to PS, which is a polymer with high electrical resistivity that can retain either positive or negative electrical charge for hours after initial charging.[20]

6.3 Experimental

6.3.1 Materials

PS, weight average molecular weight of 180,000 g/mol, and PAN, weight average molecular weight of 135,000 g/mol, were procured from Sigma Aldrich and used as such. PS was dissolved in a 90/10 (wt/wt) methylene chloride/dimethylformamide (MeCl/DMF) at a concentration of 15 wt% and PAN was dissolved separately in DMF at a concentration of 10 wt%. The solvents, MeCl and DMF were also procured from Sigma Aldrich and used as such.

6.3.2 Apparatus & Methodology

The schematic of single component (or single reservoir) and bicomponent (or dual reservoir) electrospinning apparatus are depicted in Figures 6.1 and 6.2. In both of the two apparati, a microsyringe pump from the Orion Company was used to control the throughput of the polymer solution contained in the syringes. Stainless steel plates (46 x 61 cm) were used as fiber collectors. Uncharged spunbonded polypropylene fabric was adhesively attached to the metallic collector plate in order to collect the electrospun fibers onto a substrate fabric that was easy to handle for subsequent testing for aerosol penetration and charge retention. For single component and 'layer-by-layer' spinning, plastic syringes fitted with metal needles (internal diameter, ca. 0.7 mm) were used as the polymer solution reservoir and nozzle for electrospinning. For bicomponent electrospinning, a special spinneret was utilized that was comprised of two plastic syringes adhered together, each containing a polymer solution. The narrow ends of the two syringes are connected to Teflon needles, internal diameter, ca. 0.7 mm, that are also adhered together to form a side-by-side spinneret. The microsyringe flow pump imparted the same flow rate to both the solutions emanating from each open end of the Teflon needle. For more details on the bicomponent spinneret, the reader is referred to our earlier work.[21] Power supplies (manufactured by SIMCO®) of positive and negative polarities

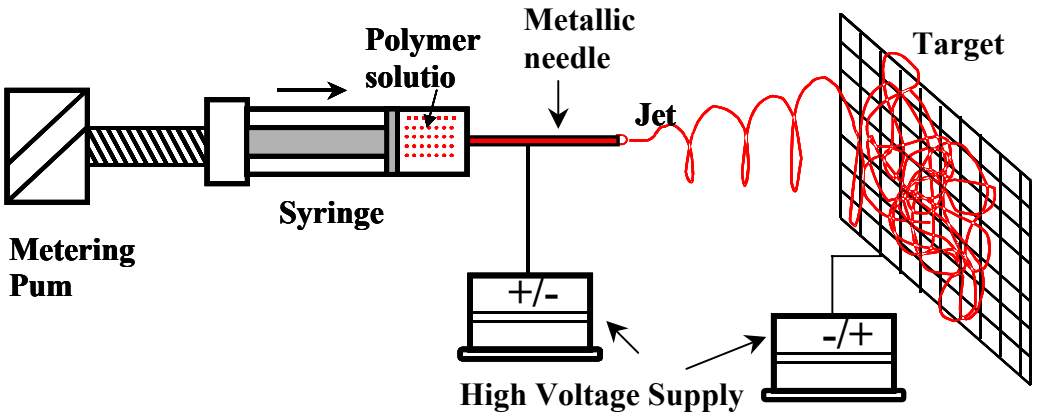

Figure 6.1 Electrospinning apparatus for 'single component' and 'layer-by-layer'

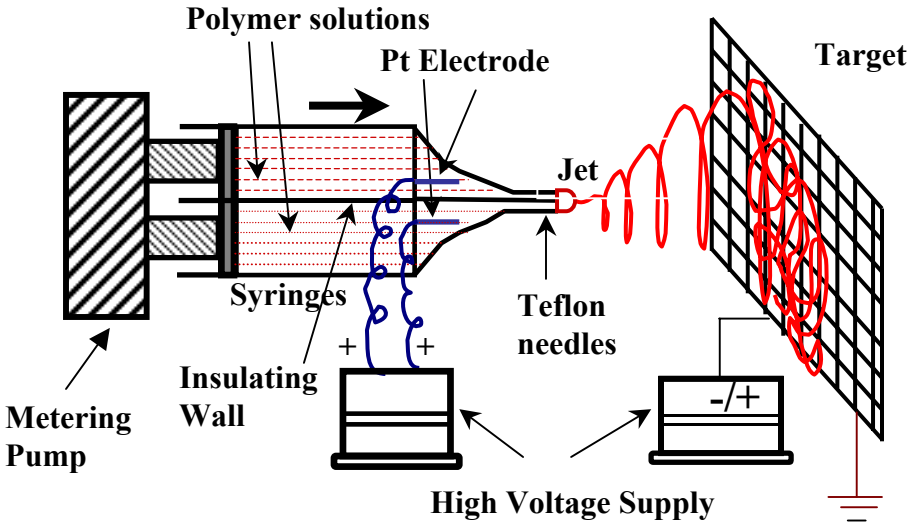

spinning.

Figure 6.2 Schematic representation of the bicomponent fiber electrospinning apparatus.

with 50 kV and 2 mA were employed as the voltage source for the electrospinning process. An electrode from one of the power supplies was used to charge the polymer solution(s) in the syringe(s), while an electrode from the second power supply was attached to the metal collector plate, held 44 cm from the charged syringe tip. Solutions of PAN, and PS were electrospun from syringes mounted on a syringe pump (Orion Co.)

+15kV respectively to maintain an overall potential drop of 30kV. Bicomponent spinning was performed at +18 kV in one case and –18 kV in another case, while keeping the collector at –12kV and +12kV respectively to maintain the overall potential drop of 30kV (same average electric field strength as that maintained for the single and multi layered electrospun configurations). The collector, covered with a spunbonded fabric, was charged with an equal charge but opposite polarity of the spinneret.

Fabrics of electrospun fibers collected on a spunbonded polypropylene (PP) were prepared in three different configurations: 1) single component fabrics of PAN and PS; 2) layer-by-layer fabrics of PAN and PS; and 3) bicomponent fabrics with blended PAN and PS fibers intermingled within the fabric. Table 6.1 shows the configurations and the surface charges delivered for each system. The PP layer was the bottom layer, followed by sequential layers of electrospun fibers. As shown in Table 6.1, PAN(+) refers to a positive PAN fiber layer on top of the PP, that was electrospun at a positive potential on the polymer solution. Likewise, PAN(+)/PS(-) designates a bottom layer of positive PAN fibers with a top layer of negative PS fibers. Four-layered fabrics are shown with the label, PS(-)/PAN(+)/PS(-)/PAN(+), designating PS on the bottom and PAN on the top of the multilayered mat. Surface charge potential measurements were made on the top, or the final layer, of charged fibers.

6.3.3 Measurements & characterization

A Leo® 1550 Field Emission Scanning Electron Microscope (FESEM) was utilized to visualize the morphology of the electrospun mat. A Cressington® 208HR sputter-coater was used to sputter-coat the electrospun fiber samples with a 10 nm Pt/Au layer to minimize the electron charging effects. In addition, infrared microscopy was conducted on a Bio-Rad© UMA 300A FTIR microscope. The 250mm Broad Band MCT allowed the samples to be evaluated from 975 to 4000 cm^{-1}. Samples in the form of small fiber segments were removed from the bulk fabric and placed on a pin hole slide while a variable aperture control was used to narrow the field of focus. These were evaluated in both the reflectance as well as the transmission mode. As the samples evaluated in the reflectance mode had a low signal to noise ratio than those tested in the transmission mode, the results reported in this study were conducted in the transmission mode.

Table 6.1 Construction and Electrospinning conditions of fabrics.

Fabric Construction (B/M/M/T)*	Potential on Solution (kV)	Potential on Target (kV)	Spinning-Time/Layer (min)
PAN(+)	+15	-15	20
PS(-)	-15	+15	20
PS(-)/PAN(+)	-15/+15	+15/-15	10 each
PAN(+)/PS(-)	+15/-15	-15/+15	10 each
PS(-)/PAN(+)/PS(-)/PAN(+)	-15/+15/-15/+15	+15/-15/+15/-15	5 each
PAN(+)/PS(-)/PAN(+)/PS(-)	+15/-15/+15/-15	-15/+15/-15/+15	5 each
PAN/PS(+):Bicomponent	+18	-12	10**
PAN/PS(-):Bicomponent	-18	+12	10**

* Bottom/Middle/Middle/Top layers. Charge polarity of each layer is indicated in parentheses.

** Bicomponent electrospinning was conducted at twice the flow rate of the layered sample, viz. 0.114 ml/min.

A capacitive probe with aperture of 0.07 inch attached to a scanning table was interfaced with an A/D board to measure the surface charge potential at 36 points across 100 cm^2 of the electrospun fabric (electrospun fibers collected on top of the spunbond polypropylene) held on the metal collector plate. After residual charge was measured, the fabric was removed from the plate and tested for aerosol penetration (AP). An aerosol generator and detector, the TSI 8130 was used to measure NaCl aerosol penetration of the electrospun fabrics. The NaCl particle had a number average diameter of 0.067 μm with geometric standard deviation of 1.6. The filtration velocity was 5.3 cm/s.

6.4 Results and Discussion

In order to compare charging and filtration results among these samples, the total layer thickness was held constant by controlling the flow rates and spin times for each layer, as noted above. PAN fibers (fiber diameter ca. 200-800 nm in diameter) were found to be significantly smaller than PS fibers (fiber diameter ca. 750 nm - 4 μm in diameter), as seen in the micrographs of Figures 6.3a & b. The diameter of the

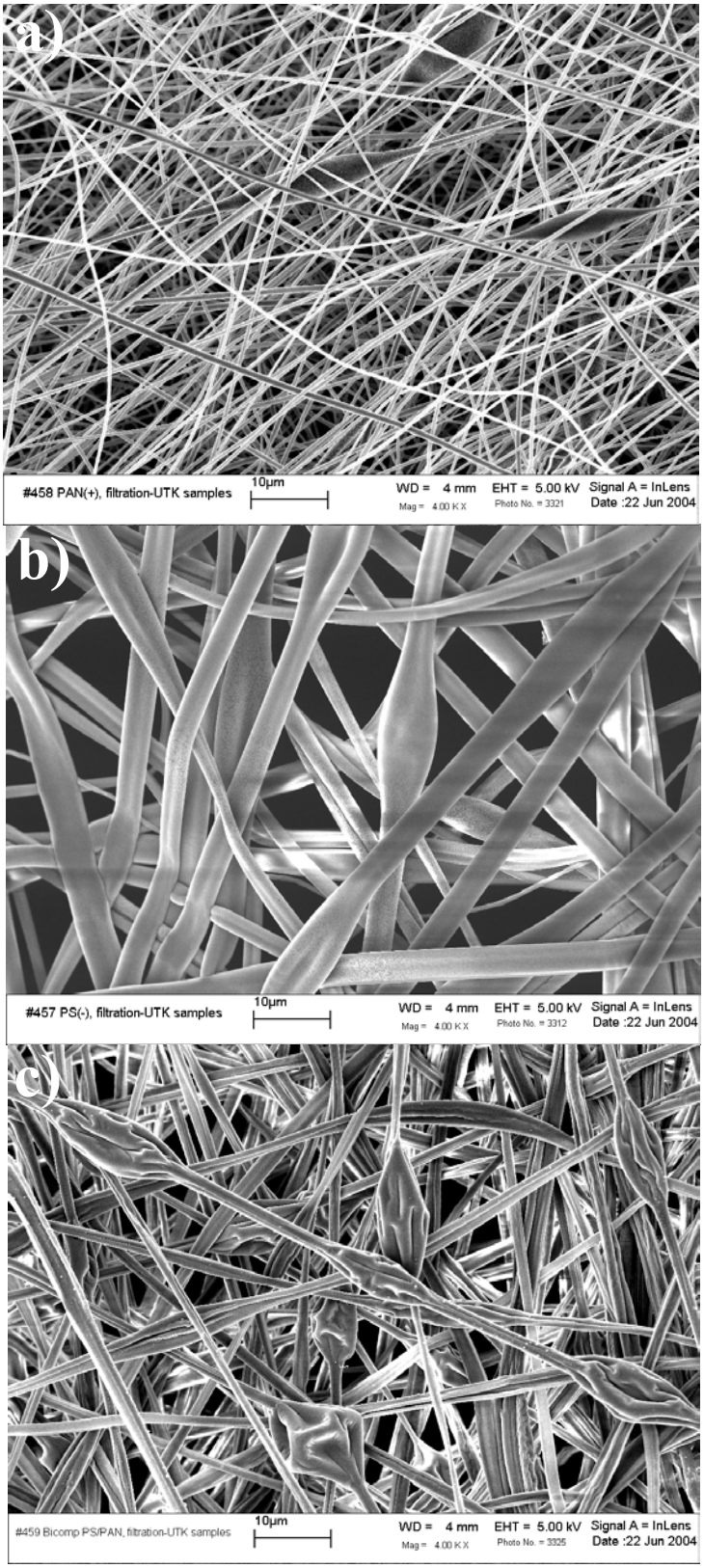

Figure 6.3 Electrospun fibers of a) PAN and b) PS fibers when spun separately (single component and layer-by-layer spinning); and c) bicomponent PAN/PS.

Table 6.2 Residual Surface Potential on Electrospun Fabrics

Fabric sample	Surface Potential After Storage Period (V)		
	10 min	**20 h**	**3 months**
PAN(+)	1950±804	1427 ±477	214 ±71
PS(-)	-3332 ±804	-2098 ±83	-40 ±48
PS(-)/PAN(+)	2042 ±771	2082 ±425	528 ±203
PAN(+)/PS(-)	-1784 ±475	-1526 ±241	16 ±2
PS(-)/PAN(+)/PS(-)/PAN(+)	2414 ±478	1290 ±70	19 ±3
PAN(+)/PS(-)/PAN(+)/PS(-)	-1587 ±441	-1150 ±122	20 ±48
PAN/PS(+):Bicomponent	1902 ±690	1122 ±275	24 ±48
PAN/PS(-):Bicomponent	-1422 ±838	-1039 ±227	-197 ±48

bicomponent PS/PAN fiber (ca. 950 nm – 2 μm, Figure 3c) was observed to be between PS and PAN fibers. In other words, the fiber diameter varied as: single component PS > bicomponent PAN/PS > single component PAN. Very high initial charge potentials were measured for all electrospun constructions, as seen in Table 6.2. Charge retention was measured at 20 hours and after 3 months of storage in ambient room air. There were no obvious trends; negatively charged surfaces did not retain more charge than positively charged surfaces. Increasing the number of charged layers (in multilayered construction) did not balance the charge or appear to stabilize the charge over time. In fact, multiple layers and bi-component fabrics seemed to lose charge as much as single fiber layers. *However, there were two samples that deviated from the others*: the samples containing two layers of either PS(-)/PAN(+) or PAN(+)/PS(-) showed a better ability to retain charge over a 20-hour period. Over the 3-month storage period, most samples lost all residual charge (values below 50 volts are not significant). However, three samples showed unusual charge retention over this extended hold period: PAN(+), PS(-)/PAN(+) and bicomponent PAN/PS(-). This set of highly charged stable samples did not suggest any trend or characteristic regarding the polarity of the surface charge, the composition of

the web, or the construction of the web as factors in the unusual stability of charge in these three cases.

The FTIR analysis on the single component PAN and PS in addition to bicomponent PAN/PS is shown in Figure 6.4. Of particular interest are the nitrile (CN) vibration at 2240 cm^{-1} in PAN[23-26] (Figure 6.4a), and the phenyl vibration at 1493 cm^{-1} in PS[27,28] (Figure 6.4b). Note that no peaks were observed at 2240 cm^{-1} in PS and at 1493 cm^{-1} in PAN respectively. This information is useful as it can be concluded that peaks corresponding to 2240 and 1493 cm^{-1} that were observed in the bicomponent PAN/PS sample (Figure 6.4c) correspond respectively to PAN and PS. This indicates that the two components are well dispersed in the bicomponent mat, indicating a significant advantage of our bicomponent electrospinning technique over the earlier attempt[20] to make uniform two-component electrospun mats.

Aerosol penetration values were measured after each storage period to determine whether there was an effect of residual charge upon the penetration levels of NaCl. The aerosol test destroys the specimen, so a set of samples different from those listed in Table 6.2, but electrospun at the same conditions as outlined in Table 6.1, were used for aerosol testing at 10 minutes and 20 hours after the samples were formed. Samples in Table 6.2 were left intact on the collector plate for the entire 3-month storage period. Samples used for aerosol tests were removed from the plates and their measured surface charges were clearly affected by handling, as seen when comparing 10 min and 20 hour data in Table 6.2 vs. Table 6.3. The % aerosol penetration is provided in Table 6.4, and the corresponding surfaces potential of these samples is reported in Table 6.3.

The bar graphs in Figures 6.5 and 6.6 (data from Table 6.3 & 6.4 respectively) depict the charge loss of all electrospun samples over time. There is a significant variance of up to 60% in the surface charge over the area of fiber measured. This variability limits any extensive interpretation of the data in these figures. We see from the graphs that the bicomponent sample that had been spun from a negatively charged solution retained a charge of nearly -200 V after three months. This was not the case for the same sample electrospun from a positively charged solution. However, this does not mean that net negative charges are stable. In the case of the one-layer PAN(+) and the two-layer system

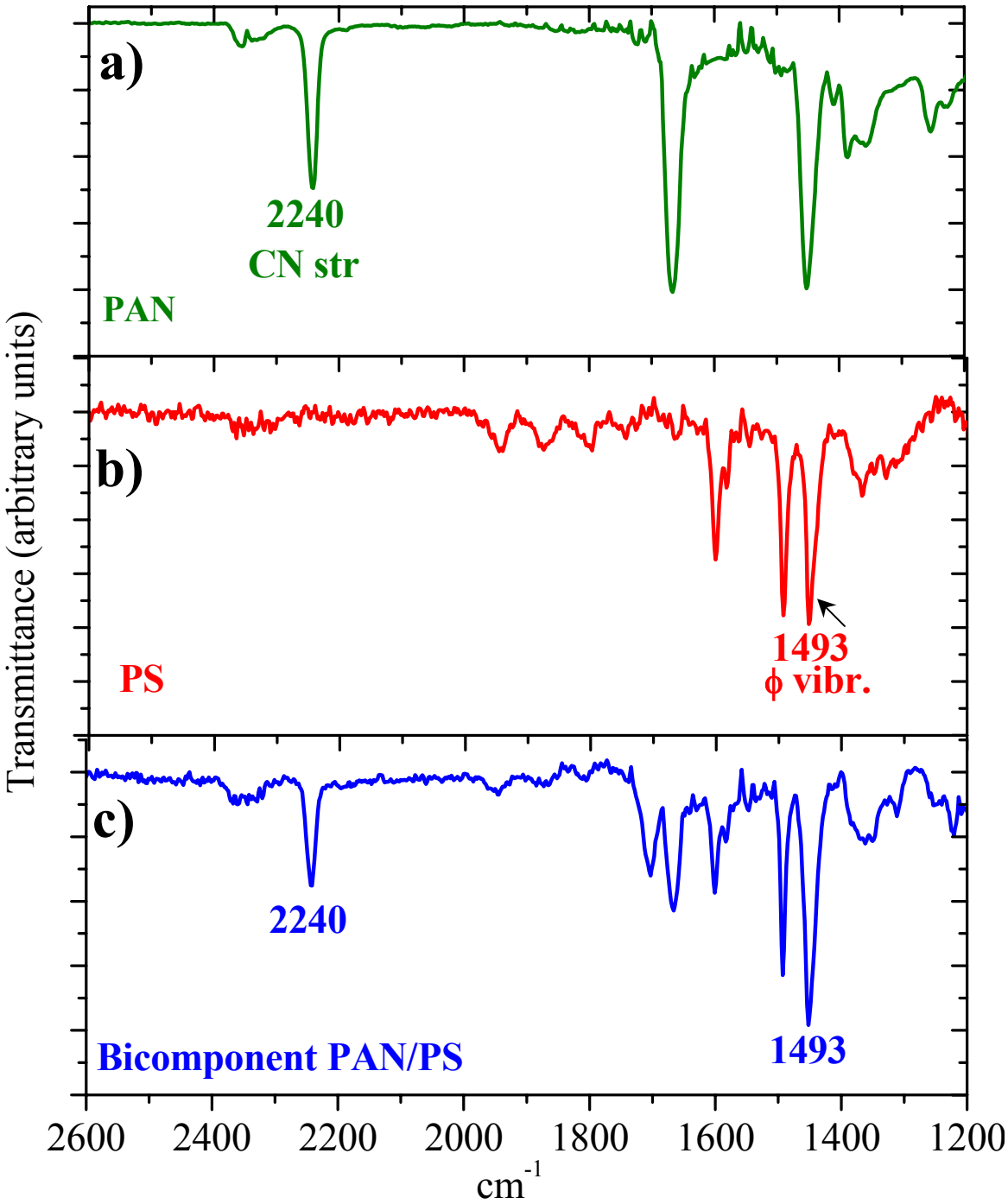

Figure 6.4 FTIR spectra of a) PAN b) PS and c) PAN/PS bicomponent fibers.

Table 6.3 Residual Surface Potential on Aerosol Test Samples

Fabric sample	Surface Potential After Storage Period (V)		
	10 min	20 h	3 months
PAN(+)	1657	-46	214
PS(-)	-1602	-229	-40
PS(-)/PAN(+)	1463	-33	528
PAN(+)/PS(-)	-1212	-164	16
PS(-)/PAN(+)/PS(-)/PAN(+)	2165	-13	19
PAN(+)/PS(-)/PAN(+)/PS(-)	-1587	-183	20
PAN/PS(+):Bicomponent	1801	1122	24
PAN/PS(-):Bicomponent	-2743	-1039	-197

Table 6.4 Aerosol Penetration of Electrospun Fabrics.

Fabric sample	% Aerosol Penetration of Electrospun Fabrics		
	10 min	20 h	3 months
PAN(+)	0.14	0.53	4.83
PS(-)	12.0	15.0	10.3
PS(-)/PAN(+)	1.20	1.70	3.10
PAN(+)/PS(-)	1.30	4.20	0.91
PS(-)/PAN(+)/PS(-)/PAN(+)	4.20	6.70	1.95
PAN(+)/PS(-)/PAN(+)/PS(-)	0.07	1.74	1.74
PAN/PS(+):Bicomponent	0.42	-	12.6
PAN/PS(-):Bicomponent	0.15	-	3.09

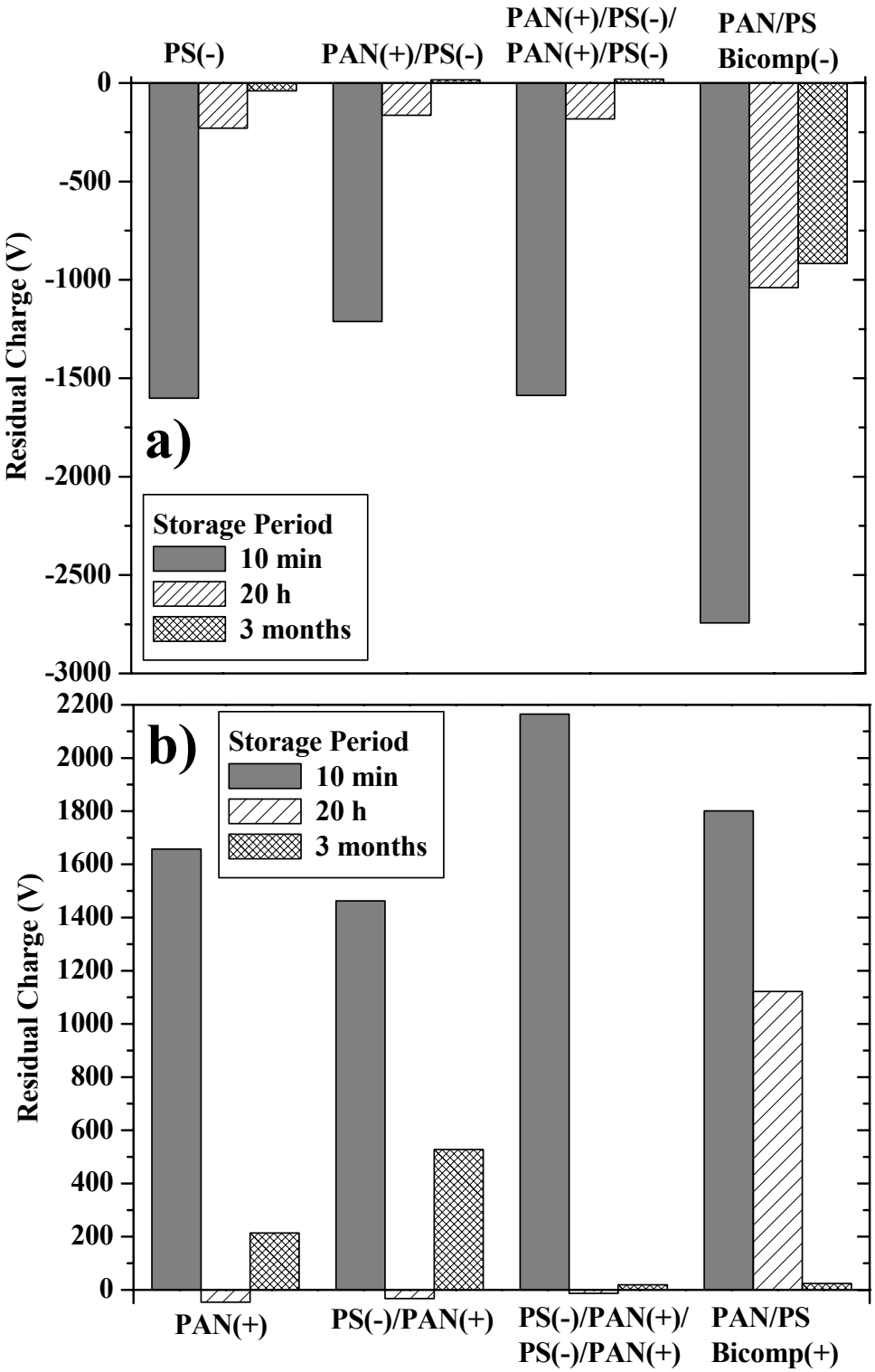

Figure 6.5 Variation of surface residual charge for a) negatively charged sample fabrics and; b) positively charged sample fabrics.

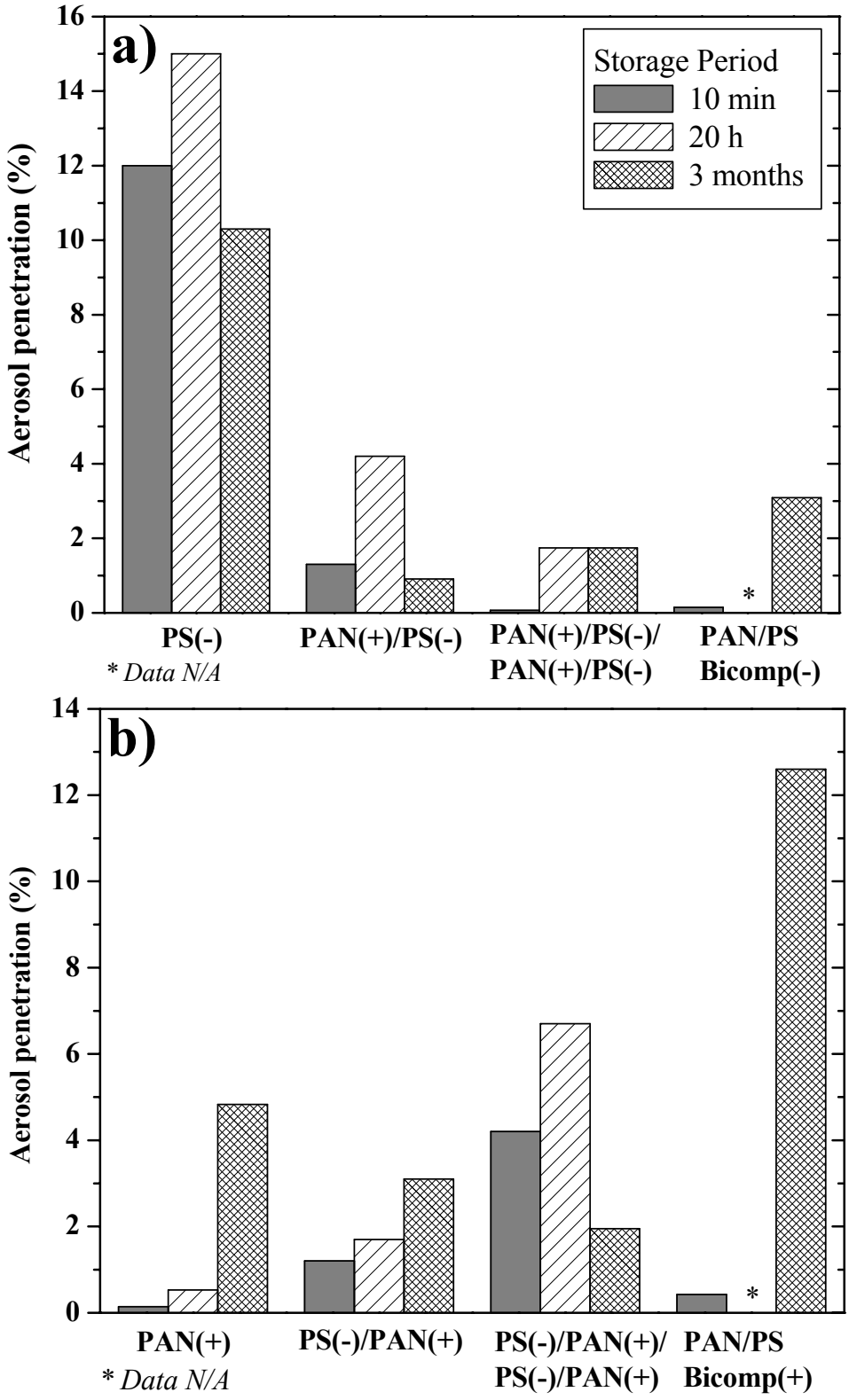

Figure 6.6 Variation of aerosol penetration for a) negatively charged sample fabrics and; b) positively charged sample fabrics.

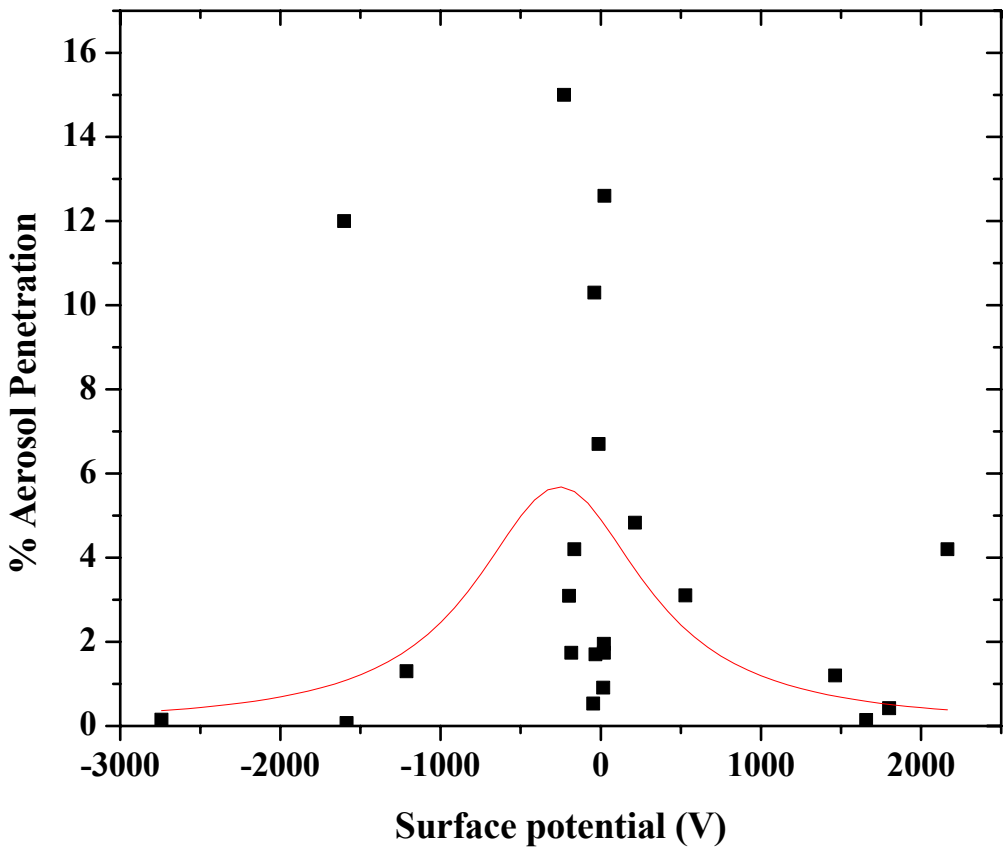

Figure 6.7 Effect of residual surface potential on aerosol penetration. The data is fitted to a Lorentz regression as indicated by the continuous line.

of PS(-)/PAN(+), we found that the positively charged one-layer and the positively charged two-layer systems retain very high charge after three months. The negative bicomponent PAN/PS(-) system retained 14% of it's charge; the positive single component PAN(+) web retained 11%, and the positive two-layer PS(-)/PAN(+) system retained 25% of it's charge. All other samples lost more than 90% of their initial charge over three months. Aerosol data of all the electrospun samples is summarized graphically in Figure 6.7. There is an apparent trend in the data showing that high surface charge on electrospun fibers generally causes lower aerosol penetration, although a few data points lie significantly outside the trend shown in Figure 6.7. Further studies would be desirable in order to confirm if this behavior of the weak dependence of aerosol penetration on the charged electrospun fibers is real.

Another important factor in aerosol penetration of nonwovens is fiber diameter. Thicker fibers produce a web with less fiber surface area that can be penetrated more efficiently by aerosol particles. Larger fiber diameters also result in lower pressure drops across the fabric during aerosol testing at constant flow rate. Data in this study, shown in Figure 6.8, confirm a weak but general trend of increasing aerosol penetration with decreasing pressure drop. In addition, when comparing the aerosol penetration of single layer PS and PAN, it can be seen that at all time intervals when the measurements were performed (10 min, 20 hour and 3 months), the aerosol penetration of PS is significantly higher than that of PAN (recall Table 6.4). Recall that the diameter of PAN fibers (ca. 200-800 nm) was found to be smaller than PS fibers (ca. 750 nm - 4 μm). This suggests that one of the web geometrical factors, viz. the fiber diameter, influences filtration properties of the electrospun fabrics.

Data in Figures 6.7 and 6.8 demonstrate a possible combined effect of fiber charge and pressure drop upon aerosol penetration, AP, (and consequently the filtration efficiency as it equals 1-AP) for electrospun fibers; a combined influence that is not apparent for other nonwovens. For traditional nonwovens, electrical charges on fabrics have been used to increase filtration efficiency with good charge retention for certain types of charging conditions including triboelectric charging of electrically dissimilar fibers and charge embedment (electret formation) in fibers.[22,29] However, the present research on finer fiber nonwovens produced by electrospinning suggests only a weak effect of charging on filtration efficiency. For melt blown fabrics, it has been shown that electrical charge will dominate the filtration behavior of charged fabrics and overcome geometrical effects, such as fabric basis weight.[30] Electrospun fabrics possess extremely fine fibers (10-100x smaller than melt blown fibers); as a result these electrospun fabrics have higher pressure drops and higher aerosol filtration efficiencies that are not substantially influenced by charge retention on the final fabric. In addition, the effect of geometrical factors such as fiber diameter is not strongly overcome by fiber charge levels.

6.5 Conclusions

In an effort to investigate the effect of electrical charges on filtration properties and to provide charge stability on the surface of electrospun fibers, we studied the effects

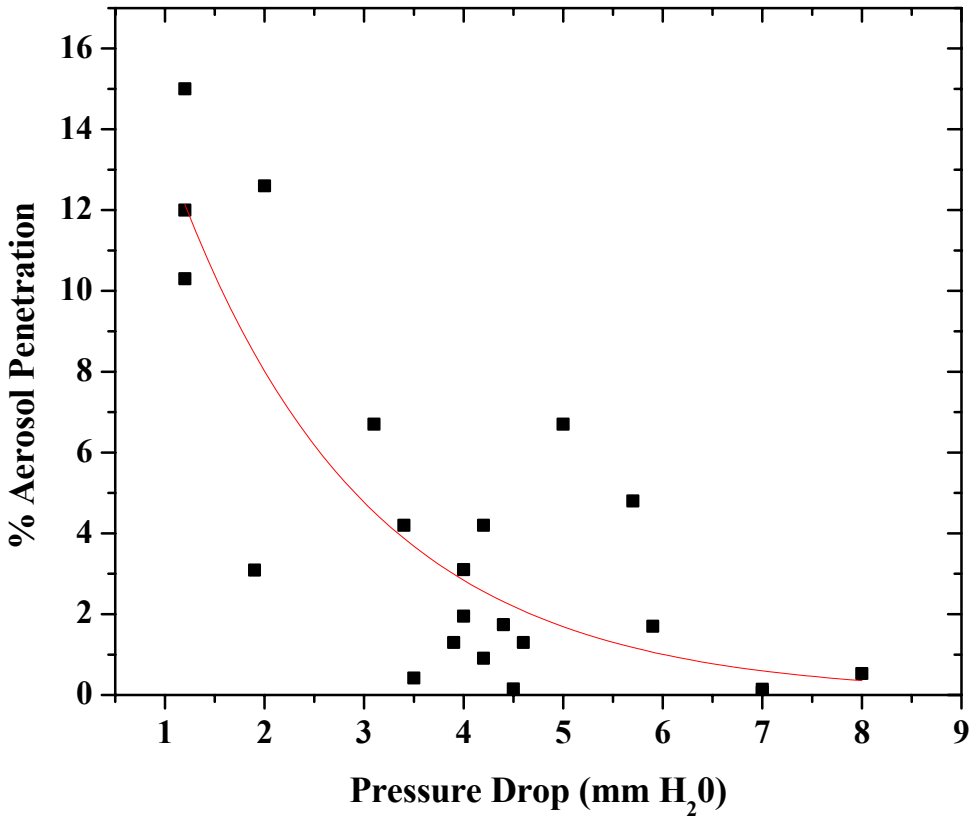

Figure 6.8 Effect of pressure drop across the electrospun fabrics on aerosol penetration. The data is fitted to an exponential decay as indicated by the continuous line.

of surface charge decay and web construction of electrically dissimilar fibers in three different configurations on filtration properties. This study demonstrated that extremely high surface charges on the fibers can result from electrospinning, and these charges diminish very little over the course of 20 hours, but are not retained over the course of three months, although three exceptions were notably charged after this long hold period. In the present investigation involving charged PAN and PS fibers, a weak relationship between electrical charge and aerosol penetration of the web was observed. Although one might expect that electrical charging of the web would overcome the influence of geometrical factors, particularly fiber diameter, on fibers investigated in this study, a dependence of the aerosol penetration on the pressure drop across the web was observed, indicating that fiber diameter influenced filtration in the presence of substantial surface

charges. Further studies need to be performed to fully define the dependence of aerosol penetration on the magnitude of charge on electrospun fibers.

Acknowledgements

This material is based upon work supported by, or in part by, the U.S. Army Research Office under grant number DAAD19-02-1-0275 Macromolecular Architecture for Performance (MAP), a multidisciplinary university research initiative project. The author thanks Phil and Heidi Gibson of the US Soldier Center, Natick MA and Prof. Peter Tsai for their collaboration on this project.

References

(1) Formhals, A.US, 2,123,992, 1934

(2) Formhals, A.US, 2,116,942, 1938

(3) Formhals, A.US, 2,109,333, 1938

(4) Formhals, A.US, 2,187,306, 1940

(5) Formhals, A.US, 2,323,025, 1943

(6) Formhals, A.US, 2,349,950, 1944

(7) Baumgarten, P. K. *J. Colloid Interface Sci.* **1971**, *36*, 71-79.

(8) Larrondo, L.; Manley, R. S. J. *Journal of Polymer Science: Polymer Physics* **1981**, *19*, 909-919.

(9) Larrondo, L.; Manley, R. S. J. *Journal of Polymer Science: Polymer Physics* **1981**, *19*, 921-932.

(10) Larrondo, L.; Manley, R. S. J. *Journal of Polymer Science: Polymer Physics* **1981**, *19*, 933-940.

(11) Doshi, J.; Reneker, D. H. *Journal of Electrostatics* **1995**, *35*, 151-160.

(12) Deitzel, J. M.; Kleinmeyer, J. D.; Hirvonen, J. K.; Beck Tan, N. C. *Polymer* **2001**, *42*, 8163-8170.

(13) Reneker, D. H.; Yarin, A. L.; Fong, H.; Koombhongse, S. *Journal of Applied Physics* **2000**, *87*, 4531-4547.

(14) Reneker, D. H.; Chun, I. *Nanotechnology* **1996**, *7*, 216-223.

(15) Shin, Y. M.; Hohman, M. M.; Brenner, M. P.; Rutledge, G. C. *Polymer* **2001**, *42*, 09955-09967.

(16) Shin, Y. M.; Hohman, M. M.; Brenner, M. P.; Rutledge, G. C. *Applied Physics Letters* **2001**, *78*, 1149-1151.

(17) Hohman, M. M.; Shin, M.; Rutledge, G.; Brenner, M. P. *Physics of Fluids* **2001**, *13*, 2221-2236.

(18) Hohman, M. M.; Shin, M.; Rutledge, G.; Brenner, M. P. *Physics of Fluids* **2001**, *13*, 2201-2220.

(19) Hinds, W. C. *Aerosol Technology - Properties, Behavior, and Measurement of Airborne Particles, Chapter 9*, 2nd ed.; John Wiley & Sons, Inc.: NY, 1999.

(20) Tsai, P.; Schreuder-Gibson, H. L. *INTC 2003, International Nonwovens Technical Conference, Conference Proceedings, Baltimore, MD, United States, Sept. 15-18, 2003* **2003**, 403-413.

(21) Gupta, P.; Wilkes, G. L. *Polymer* **2003**, *44*, 6353-6359.

(22) Smith, P. A.; East, G. C. *Journal of Electrostatics* **1988**, *21*, 81-98.

(23) Dalton, S.; Heatley, F.; Budd, P. *Polymer* **1999**, *40*, 5531-5543.

(24) Fennessey, S. F.; Farris, R. J. *Polymer* **2004**, *45*, 4217-4225.

(25) Bashir, Z.; Church, S.; Waldron, D. *Polymer* **1994**, 967.

(26) Bashir, Z.; Atureliya, S. K.; Church, S. P. *Journal of Materials Science* **1993**, *28*, 2721-2732.

(27) Brack, H. P.; Fischer, D.; Peter, G.; Slaski, M.; Scherer, G. G. *Journal of Polymer Science, Part A: Polymer Chemistry* **2003**, *42*, 59-75.

(28) Colthrup, N. B.; Daly, L. H.; Wiberley, S. E. *Introduction to Infrared and Raman Spectroscopy, Chapter 8*, 3rd ed.; Academic: San Diego, CA, 1990.

(29) Tsai, P. P.; Wadsworth, L. C. *TAPPI Journal* **1998**, *81*, 274.

(30) Tsai, P. P.; Wadsworth, L. C. *Advances in Filtration and Separation Technology, American Filtration and Separation Society* **1995**, *9*, 473.